Pergamon

PII: S0967-0637(96)00122-7

Deep-Sea Research I, Vol. 44, No. 6, pp. 1025–1054, 1997

0967-0637/97 $17.00 + 0.00

Mid-depth ventilation in the western boundary current system of the sub-polar gyre

ROBERT S. PICKART,* MICHAEL A. SPALL* and JOHN R. N. LAZIER†

(*Received* 24 *May* 1995; *in revised form* 27 *March* 1996; *accepted* 5 *September* 1996)

Abstract—Two processes are investigated that result in the rapid (order of months) export of newly-ventilated water from the sub-polar north Atlantic. Both mechanisms involve mid-depth water mass formation within the western boundary current system, which leads to such rapid spreading. The first mechanism, which apparently occurs every winter, forms upper Labrador Sea water (LSW), which is a source of the high CFC layer of the upper deep western boundary current (DWBC). A mixed-layer model shows that this water mass can be formed by convection in the main branch of the Labrador Current. Strong heat loss near the boundary together with the existing potential vorticity structure of the current enables overturning to 1000 m. A regional numerical model of the circulation near Flemish Cap reveals how eddies of upper LSW are then shed by the baroclinically unstable Labrador Current. The eddies become detached from the boundary at the entrance to Flemish Cap and are entrained in to the offshore (barotropic) branch of the Labrador Current, which brings them seaward of Flemish Cap (where they have been previously observed). The second mechanism presented occurs only under extreme winter forcing, such as that experienced in the Labrador Sea in recent years. The enhanced heat loss forms classical LSW south of the cyclonic gyre, where the DWBC and North Atlantic Current can then quickly transport the water away from the Labrador Sea. It is shown that newly-ventilated lenses of classical LSW observed in the DWBC likely originate from this southern region, consistent with their sudden appearance downstream in the early 1990s. © 1997 Elsevier Science Ltd

INTRODUCTION

The western boundary current system in the North Atlantic sub-polar gyre is very complex and plays a critical role in the meridional overturning circulation of the global ocean. It consists of both wind-forced and buoyancy-driven currents throughout the water column, which strongly influence the net meridional fluxes of mass, heat, freshwater and tracers. These in turn impact the strength of the meridional overturning and the net production of new water. In recent years conditions in the western sub-polar gyre have changed significantly at mid-depth, characterized by substantial cooling of intermediate waters (e.g. Koltermann, 1995). This is partly the result of a series of harsh winters in the western basin, and it signifies the importance and impact of local climate forcing on the system.

The ventilation of the North Atlantic is intimately tied to the modification and export of waters in the western boundary region of the sub-polar gyre. The dominant currents that transport water to the sub-tropics are the Labrador Current and Deep Western Boundary Current (DWBC). The former is well known for carrying cold, fresh water on the shelf and

* Woods Hole Oceanographic Institution, Woods Hole, MA 02543, U.S.A.
† Bedford Institute of Oceanography, Dartmouth, Nova Scotia, Canada, B2Y 4A2.

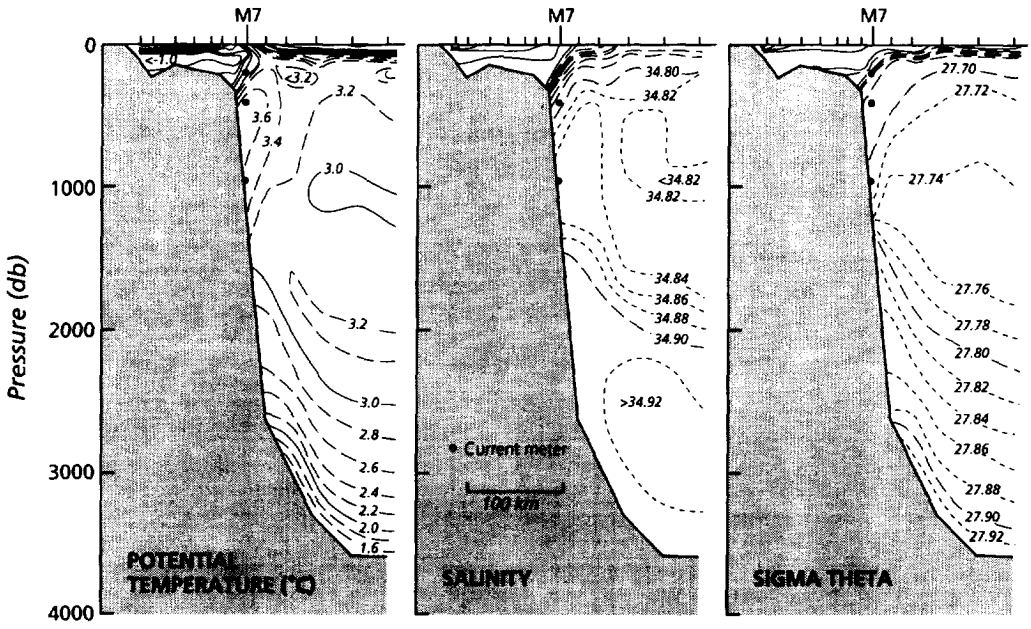

Fig. 1. Vertical section of (left) potential temperature, (centre) salinity, and (right) potential density across the western Labrador Sea, after Lazier and Wright (1993). The location of the section corresponds roughly to that of the northern-most line in Fig. 2. The main branch of the Labrador Current is evident as the front near the shelf break, and the mooring located within this current (discussed in the Results) is denoted M7.

upper slope, while the latter advects recently formed deep and bottom waters southward. In this paper we discuss various elements of the ventilation in the region—involving both these currents—which appear to play an important role in the replenishment of subthermocline waters of the mid-latitude Atlantic. Our first topic involves a process that apparently occurs every year (though it has not been previously investigated), while the second process we consider seems to occur only in cases of extreme atmospheric forcing.

The main branch of the Labrador Current is situated near the shelf break; its surface waters are extremely cold and fresh (originating partly from Baffin Bay and Hudson Strait) (Lazier and Wright, 1993) and there is a strong front associated with the flow (Fig. 1). This current continues southward through Flemish Pass to the Grand Banks of Newfoundland, where at least part of it retroflects eastward. Recently Lazier and Wright (1993) have reported observations of another southward jet situated just offshore of the main Labrador Current, centered on the 2500 m isobath. This flow is nearly barotropic (hence does not have a baroclinic signature in density) with a vertically averaged speed of roughly 15 cm s^{-1}. It is believed to be part of the wind-driven return flow of the sub-polar gyre, consistent with the Sverdrup transport calculations of Thompson *et al.* (1986). Lazier and Wright (1993) refer to this jet as the "deep" Labrador Current. Pickart *et al.* (1996) have observed a comparable barotropic flow to the south, seaward of Flemish Cap. Offshore of the deep Labrador Current resides the equatorward flowing DWBC. This bottom intensified flow (which does have a density signature, Fig. 1) transports recently formed Norwegian–Greenland overflow water, whose high-oxygen core is situated at roughly 3000 m.

The circulation along the western boundary of the sub-polar gyre thus includes three dynamically distinct currents from the shelf break to the base of the continental slope. Further offshore, in the Labrador Sea proper, is a weaker cyclonic circulation characterized by a doming of isopycnals towards the center of the basin. Within this gyre is a thick layer of nearly homogeneous water extending to roughly 2000 m, which is known as classical Labrador Sea water (LSW, e.g. Lazier, 1973). The western edge of this layer is evident in Fig. 1. This water is formed by deep convection during winter, though the depth of the overturning and the T–S of the final water mass product vary extensively both inter-annually and decadaly (see Lazier, 1980; Talley and McCartney, 1982; Lazier, 1988). Using historical data, Talley and McCartney (1982) revealed three primary spreading routes of the classical LSW away from the Labrador Sea based on its low potential vorticity signal: (i) to the northeast into the Irminger basin; (ii) to the southeast into the interior North Atlantic; and (iii) equatorward along the western boundary in the DWBC (above the Norwegian–Greenland overflow water). Based on more recent mid-latitude data from the 1980s, this latter path seems to have been essentially shut off for an extended period (see Pickart *et al.*, 1996).

This paper has been inspired by two recent observations in the sub-polar gyre reported by Pickart *et al.* (1996) using data collected in 1991. The first is the discovery of mid-depth sub-mesoscale eddies of newly-ventilated water found over the continental slope to the northeast of the Grand Banks. Pickart *et al.* (1996) describe in detail one such feature embedded in the deep Labrador Current. These eddies were observed in winter and carry water that is anomalously cold and fresh, weak in stratification and high in CFC content (suggesting convective origin). This water mass is distinct from classical LSW; hence Pickart *et al.* (1996) have termed it "upper" LSW (as it is found at shallower depths). The eddies erode within months, which explains why they have not been commonly observed, and are a source of the mid-depth high-CFC signal observed along the western boundary throughout the North Atlantic (see Pickart, 1992). The second intriguing observation reported by Pickart *et al.* (1996) is the presence of newly-ventilated classical LSW in the DWBC (deeper than the aforementioned sub-mesoscale eddies). Throughout the 1980s no newly-ventilated classical LSW was detected in the DWBC. Since the 1991 cruise, however, more deep lenses have been observed, and as of fall 1994 this layer of the DWBC was nearly full of such newly-ventilated water along the mid-Atlantic Bight.

The specific questions we aim to answer in this paper are: (1) What is the source of the water in the mid-depth sub-mesoscale eddies (i.e the water that ultimately helps form the mid-latitude CFC signal)? (2) How are these eddies formed? and (3) What has led to the abrupt appearance of deeper classical LSW downstream in the DWBC? We begin by presenting lateral property sections constructed from the combined hydrographic data set of Pickart *et al.* (1996) along the western boundary of the sub-polar gyre. These indicate that the upper LSW does not originate in the central Labrador Sea. Next we apply a mixed-layer model to historical T–S data from the Labrador basin to investigate the different wintertime water mass products of the region. This reveals that the upper LSW can be formed by convection at the western boundary of the Labrador Sea within the main branch of the Labrador current, an assertion supported by *in situ* wintertime current meter data. We then implement a regional numerical model of the two branches of the Labrador Current, which demonstrates how upper LSW eddies are formed by the baroclinic branch of the current and subsequently become entrained into the neighboring barotropic jet. Finally, the mixed-layer model is used to demonstrate how particularly harsh winter conditions can form classical

LSW that has a more direct route in to the DWBC, a scenario that is consistent with the recent observations. Our results together highlight different aspects of the sub-polar ventilation process that have important basin–scale ramifications, particularly with regard to the timescales and pathways of spreading.

LATERAL SECTIONS

A combined data set from two hydrographic cruises (winter 1991, spring 1992) along the western boundary of the sub-polar gyre has been assembled by Pickart *et al.* (1996). We have added a section from a third cruise (spring 1991), which then provides nearly continuous coverage of the western boundary from the mid-Labrador Sea to 55°W (Fig. 2). The cruises were R.V. *Endeavor-223* (March 1991), C.S.S. *Hudson-92014* (June 1992) and C.S.S. *Hudson-91007* (May 1991). Details of the former two are given in Pickart *et al.* (1996). The data from the last cruise include bottle salinity (though the accuracy and sampling resolution are sufficient for our purposes).

The favorable resolution of the hydrographic measurements in Fig. 2 offers a good

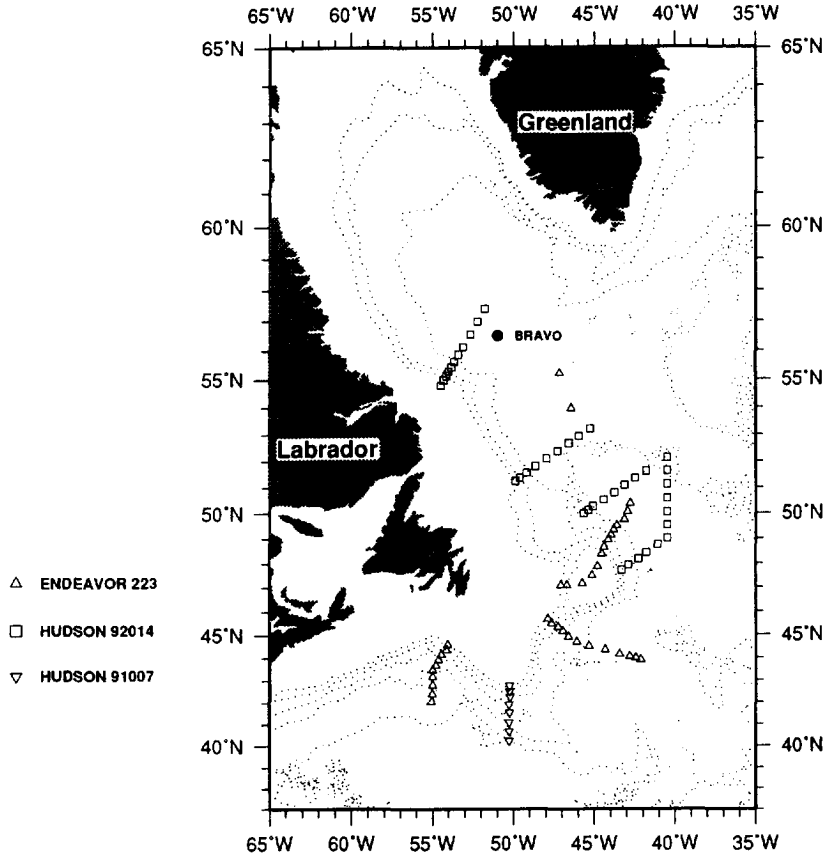

Fig. 2. Combined hydrographic data set used in the study, from three cruises in the western sub-polar gyre in 1991–1992 (see text). Also shown is the location of Ocean Weather Ship *Bravo*.

opportunity to construct lateral property maps. These provide a valuable snapshot of conditions in the western sub-polar gyre in the early part of this decade. We present maps in two density layers: $\sigma_\theta = 27.75$–27.78 kg/m^3, which is the layer of the classical LSW and $\sigma_\theta = 27.68$–27.72 kg/m^3, which corresponds roughly to the upper LSW. Figure 3 contains the lateral maps of potential temperature averaged in these two layers. In both maps the North Atlantic Current is evident as the warm region to the southeast (indicated as well by the deepening isopycnals of the front, see Fig. 5). Equatorward of the Grand Banks the slope water temperatures have moderated, most likely due to mixing with the nearby Gulf Stream (located south of the map). In the region north of 45°N, the two maps exhibit a fundamental difference. The lower layer exhibits a generally smooth transition from warmer to colder water as one progresses northward into the Labrador Sea (Fig. 3(a)). In contrast, the shallow layer shows an isolated area of cold water located in the vicinity of Flemish Cap (Fig. 3(b)). This is due to the presence here of the upper LSW eddies discussed in Pickart *et al.* (1996). (The signal from the individual eddies has been smoothed due to the contouring.)

The implication here is that the classical LSW has its origin in the interior Labrador Sea (Fig. 3(a) implies southward spreading via the boundary current system and moderation to higher temperatures due to mixing along the way). However, it is diffcult to imagine that the upper LSW is similarly spreading southward from this region (Fig. 3(b)), because of the area of higher temperature immediately south of the Labrador Sea (which isolates the cold upper LSW near Flemish Cap). The notion of simple southward advection and mixing is deficient in explaining this distribution. This suggests that the upper LSW does not originate in the same geographical area as the classical LSW.

This idea is further strengthened by considering the lateral maps of layer thickness (Fig. 4) and upper interface depth of the density layer (Fig. 5). We note that layer thickness is nearly equivalent in this context to potential vorticity (i.e. the beta effect is small compared with observed variations in layer thickness). In the deeper layer one sees a strong trend of increasing layer thickness progressing into the Labrador Sea to values greater than 1500 m (Fig. 4(a)). This is the signature of the homogeneous layer of classical LSW which occupies the bulk of the central Labrador Sea (discussed in the Introduction). The thickness map of the shallower layer (Fig. 4(b)) again shows anomalous values in the vicinity of Flemish Cap. This is due to the large thickness of the upper LSW eddies, corresponding to their reduced stratification (discussed in Pickart *et al.*, 1996). Note that nowhere to the north in the shallow layer are values as large as this, and in the interior Labrador Sea, thicknesses are less than 100 m. In this region the upper interface of the shallower density layer resides just below the sea surface (< 100 m, Fig. 5(b)). Hence, water of this density occupies only a thin near-surface layer in the Labrador Sea (recall that the data were collected during late-spring). During winter cooling the layer here will rapidly vanish (see section 3.2), precluding this locale from being the source of the upper LSW. This also implies that the winter outcrop line of this layer will occur to the south, somewhere within the area of higher temperature in Fig. 3(b) (discussed above); thus the upper LSW cannot also be formed on the southern fringes of the Labrador Sea. In the deeper layer the upper interface is also located at fairly shallow depths in the Labrador Sea (300–400 m, Fig. 5(a)). This is presumably a reflection of the fact that this layer was in contact with the atmosphere earlier in the winter season.

It is thus evident from these lateral maps that while the classical LSW seems to originate from the central Labrador Sea, the upper LSW cannot. In the next section we use a mixed-

layer model to investigate the wintertime cooling in the region, in order to determine where the upper LSW is formed.

WINTER WATER MASS PRODUCTS

Direct observation of deep convection in the central Labrador Sea has been very limited. This is due in part to the small scales of the overturning as well as the difficulty in obtaining wintertime measurements in the Labrador Sea. None the less, mixed layers of classical LSW as deep as 2000 m in the interior Labrador Sea have been observed. For example, Clarke and Gascard (1983) witnessed convection in the winter of 1976, and Wallace and Lazier (1988) observed a similar deep homogeneous layer in 1986. Using a mixed-layer model, Clarke and Gascard (1983) demonstrated how this water can be formed via overturning. Briefly, surface water which recirculates in the cyclonic gyre of the Labrador Sea, subject to typical wintertime buoyancy flux, becomes dense enough by late winter to convect as deep as 2000 m. In this section we apply the mixed-layer model of Clarke and Gascard (1983) to a winter hydrographic data set collected in February 1978 (Fig. 6). The winter of 1978 was particularly mild, so these data are reflective of typical early winter conditions (prior to overturning). As such we use them as input to the model. Because of the anomalous northeasterly winds associated with the mild conditions in 1978, measurements could be taken well on to the shelf, which is typically ice-covered by February. This provides broad spatial coverage for which to look for various water mass products in the region (note that our recent data set of Fig. 2 does not in general extend to the shelf break).

Mixed-layer model

We used the one-dimensional version of the Clarke and Gascard (1983) model (details of which are described in their paper). The mixed-layer is forced by heat loss and evaporation, and when the layer becomes statically unstable it mixes with enough underlying water to become stably stratified again, hence forming a deeper mixed-layer. The model was implemented at each location in Fig. 6 using the associated T and S profiles as the initial state. It is worth noting that the purpose of this exercise is simply to determine the general T–S characteristics of the wintertime water mass products formed in this region; particularly to see if we are able to produce a water type consistent with the upper LSW observed downstream by Pickart *et al.* (1996). Clearly there are more sophisticated mixed-layer models that could be invoked, but at this point we are not pursuing the detailed physics of the transformations but starting with the first step of determining general water classes. The encouraging results shown below demonstrate that further study is needed to investigate the precise formation processes; an important topic for future work.

We forced the model using a climatological average time series of net heat flux from Ocean Weather Station *Bravo* (Fig. 7(a); M. Visbeck, personal communication). As *Bravo* is located at the offshore edge of the domain (Fig. 6), spatial variation was accounted for as follows. First, monthly averaged ECMWF heat flux maps were obtained for a 3-year period for the region of the Labrador Sea (Caruso *et al.*, 1995). The wintertime distribution contains a strong front which roughly parallels the shelf break. This corresponds with the ice edge (hence reduced flux, see also Moore, submitted), which in turn is associated with the main branch of the Labrador Current: onshore of the current's salinity front the fresh surface water freezes, while offshore it typically does not. Since the mixed-layer model

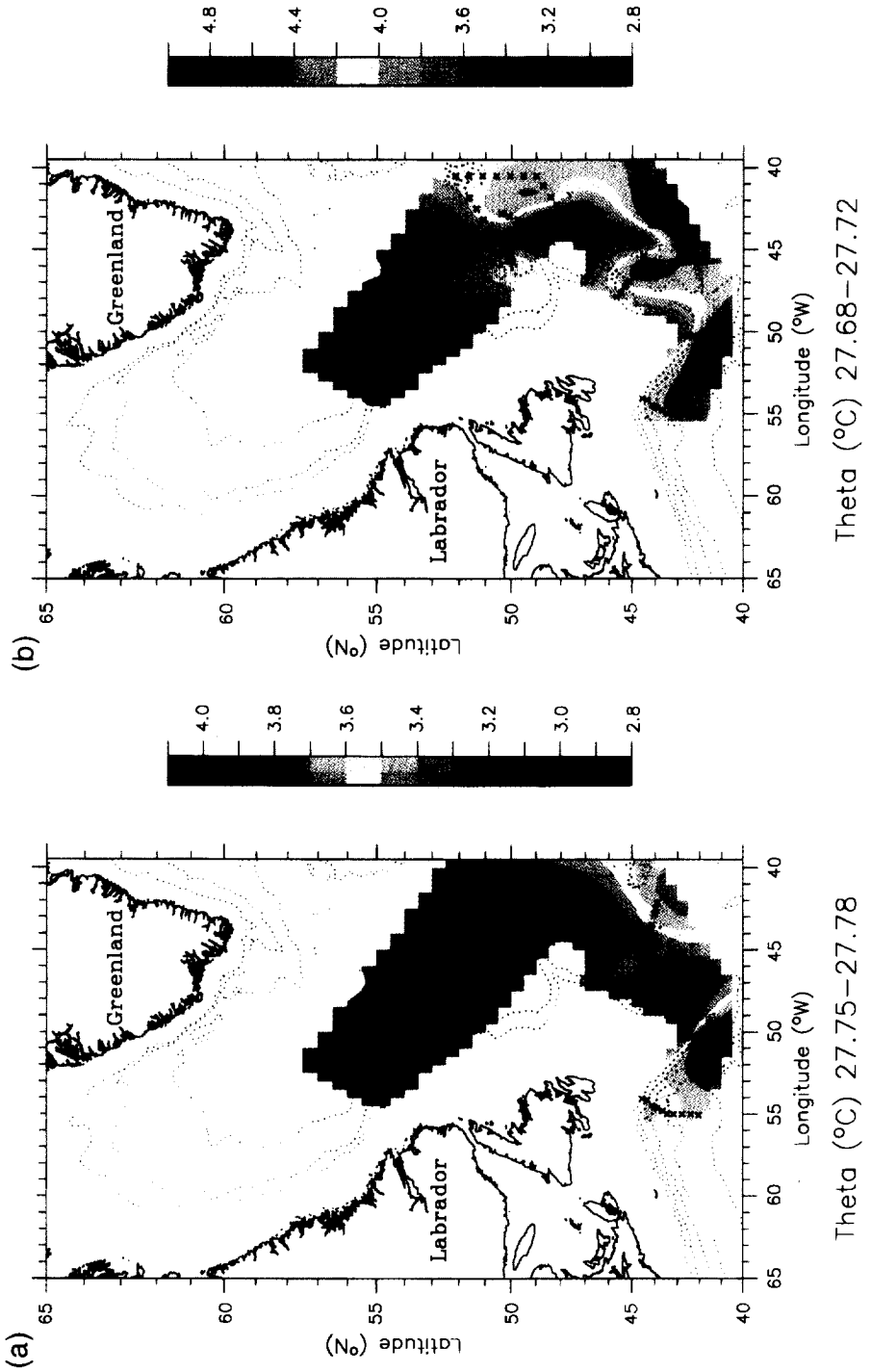

Fig. 3. Lateral distribution of potential temperature averaged within density layers (data points marked by xs). (a) Layer corresponding to classical LSW, $\sigma_\theta = 27.75$–27.78 kg/m^3. (b) Layer corresponding to upper LSW, $\sigma_\theta = 27.68$–27.72 kg/m^3.

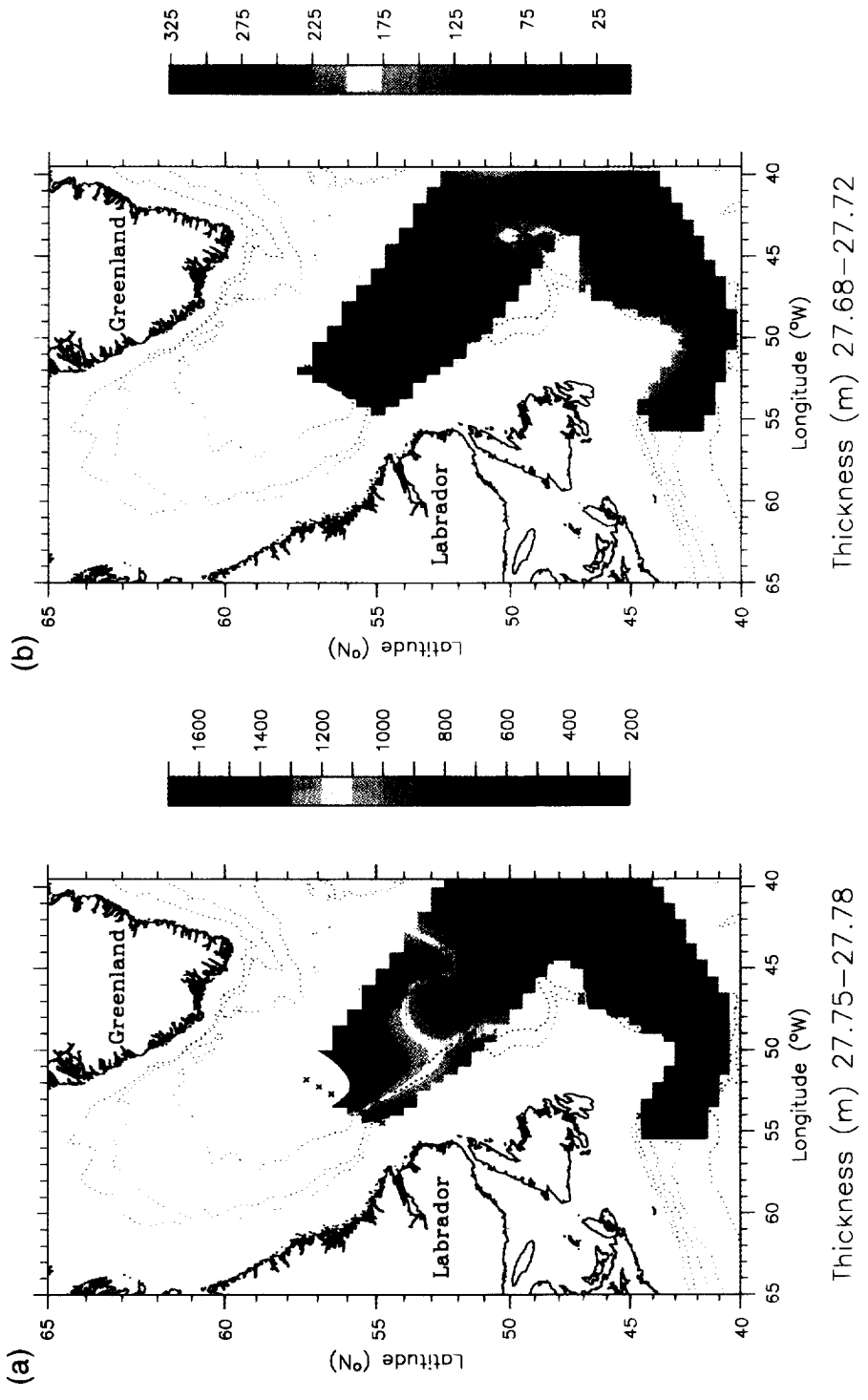

Fig. 4. Thickness of the density layers in Fig. 3. (a) Classical LSW layer. (b) Upper LSW layer.

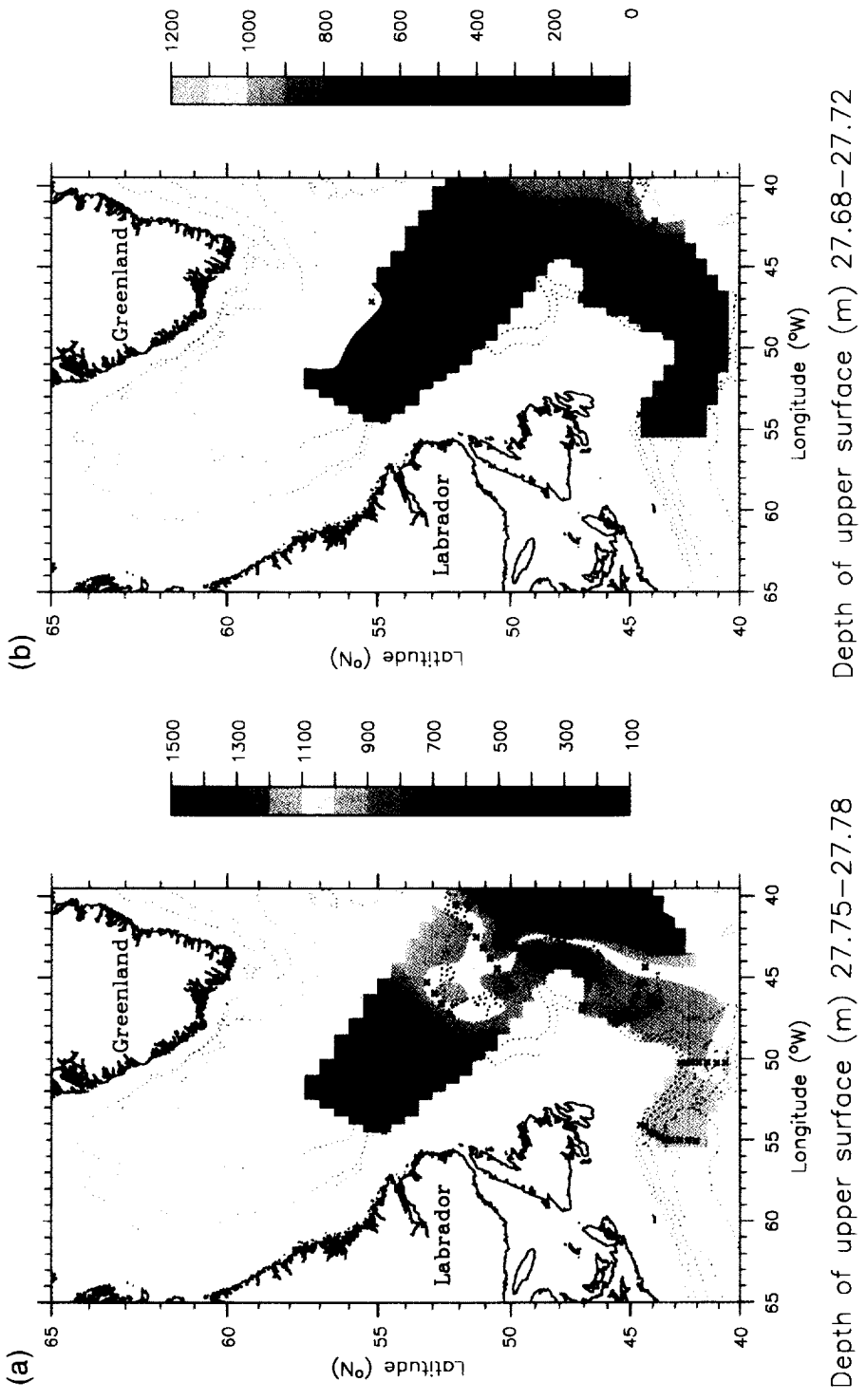

Fig. 5. Depth of the upper interface of the density layers in Fig. 3. (a) Classical LSW layer. (b) Upper LSW layer.

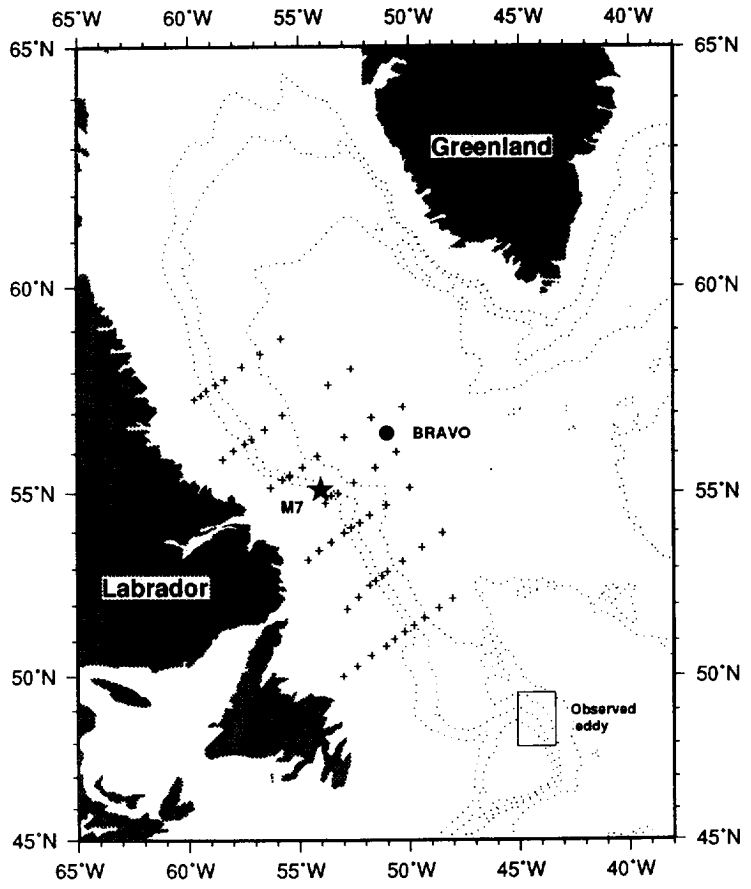

Fig. 6. Locations of the winter hydrographic stations used in the mixed-layer analysis (seven sections, where section 1 is the southern-most line). The position of Ocean Weather Ship *Bravo* is indicated, as is the location of mooring M7 in the Labrador Current. The large open rectangle denotes the site where the upper LSW eddy was observed in winter 1991, as described by Pickart *et al.* (1996).

accounts for such reduced flux when ice forms, we removed this front from the ECMWF heat flux maps by simply extrapolating the adjacent offshore values on to the shelf. Next, each map was normalized relative to the value at the *Bravo* site, and the average winter-distribution was then constructed (Fig. 7(b)). This distribution shows a pool of maximum heat loss in the northwest Labrador Sea, with decreasing values offshore and to the south (roughly a 40% variation). At each station we applied the *Bravo* heat flux time series modulated by the appropriate normalization factor in Fig. 7(b). The rationale here is that the *in situ Bravo* time series is more accurate than the model-derived ECMWF temporal evolution. However, the consistency of the ECMWF winter distribution over the 3-year period implies that the spatial information so provided is meaningful (though results presented below are not overly sensitive to this spatial variation).

Similar time-series information regarding precipitation does not exist thus we used the constant evaporation rate employed by Clarke and Gascard (1983). This is not a problem

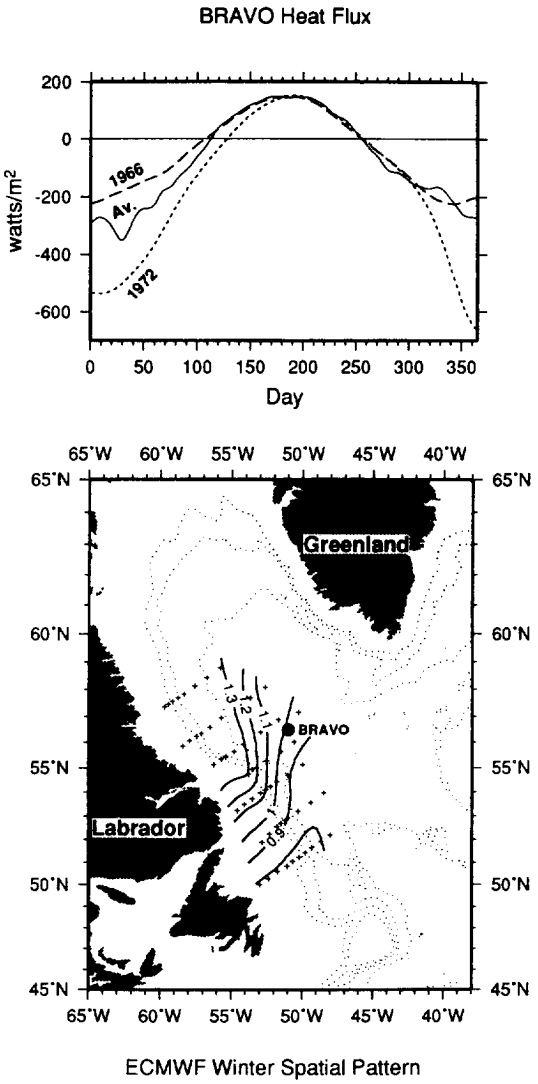

Fig. 7. (top) Time series of total heat flux observed at Ocean Weather Ship *Bravo* (M. Visbeck, personal communication). The solid curve denotes the climatological average over the period 1964–1974. The extreme winters of 1966 (weak) and 1972 (strong) are also shown (subject to a low-pass filter of 100 days). (bottom) Spatial distribution of total heat flux over the domain of Fig. 6 from ECMWF, normalized to the value at *Bravo*. This represents a 3-year winter average (1986–1988), where the near-shore ice-front has been removed (see text).

because in the context of a complete seasonal cooling period, variations in the precipitation are unimportant (recall that the purpose of the model was to estimate the final winter T–S products, not the details of convective events). The model was run for the January–April cooling period (Fig. 7(a)), and in all cases the mixed-layer variables began approaching an asymptote, signifying a robust winter product.

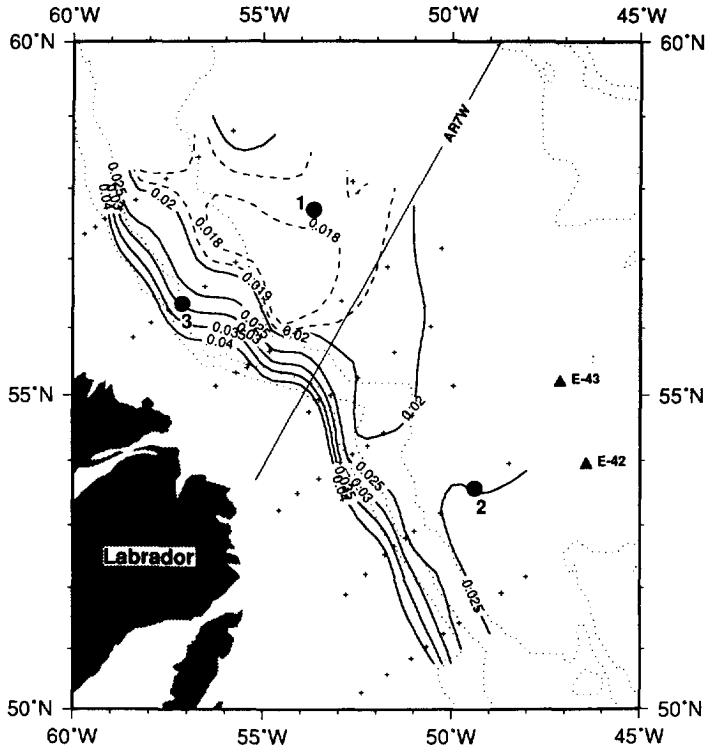

Fig. 8. Averaged dynamic height over the top 100 db (relative to 100 db) using the winter data set of Fig. 6. Three distinct dynamical regimes are associated with the three different water mass products (see text). The representative station for each regime (Fig. 9) is marked by a solid circle. Also shown are the location of the annual AR7W hydrographic line and the two EN223 stations in the southern Labrador Sea occupied in 1991.

Results

The mixed-layer water mass products can be roughly divided into three categories. These correspond to separate geographical, as well as dynamical, regions (excluding the shelf): (1) the northern interior; (2) southern interior; and (3) a narrow band along the upper continental slope (Fig. 8). Dynamically, region 1 corresponds to the western Labrador Sea cyclonic gyre where Clarke and Gascard (1983) observed the newly-formed classical LSW in winter 1976. Region 2 is characterized by weak flow adjacent to the western boundary, and the beginnings of an anti-cyclonic drift further offshore. Region 3 corresponds to the seaward edge of the main branch of the Labrador Current. Figure 9 shows the time history of mixed-layer depth and its evolution in θ–S space for a representative station in each of the three regions (Fig. 8 shows the locations of the three stations).

Classical LSW. The northern region is where classical LSW is formed. This was to be expected based on our lateral maps and on earlier work (e.g. Clarke and Gascard, 1983). The mixed-layer depth in this region reaches 1500–2000 m, and the final θ–S product is comparable with the value observed at the northern end of our lateral maps for this layer (see above). Note in Fig. 9(b) that the density of the mixed-layer quickly increases beyond

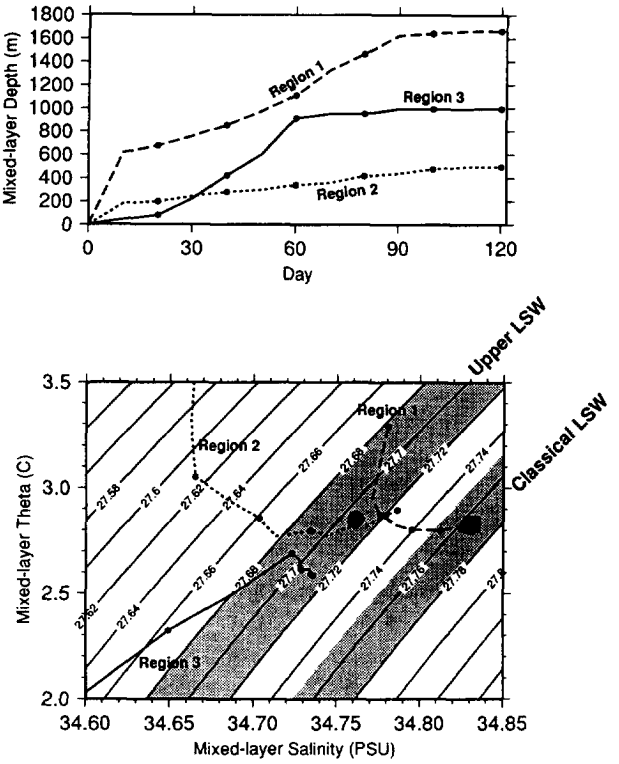

Fig. 9. Temporal evolution of the mixed-layer in the three different regions of Fig. 8. (a) Time series of mixed-layer depth, where the dots denote 20-day intervals. (b) Evolution of the mixed-layer in θ–S space. The density ranges of the upper LSW and classical LSW are indicated by shading. The large circle denotes the θ–S of the upper LSW eddy observed downstream by Pickart *et al.* (in press). The large square is the average θ–S at the northern edge of the classical LSW layer in Fig. 3(a).

the range of the upper LSW (on the order of 20 days), which confirms our earlier conjecture that the thin upper layer of lighter water in the central Labrador Sea gets eroded immediately at the onset of cooling. Depending on the strength of the forcing there is variation in the final overturning depth of the classical LSW. For the station shown in Fig. 9, the difference in mixed-layer depth between the strong and weak forcing cases of Fig. 7(a) is 1000 m. This is reminiscent of the large inter-annual variation in mixed-layer depth observed at *Bravo* as reported by Lazier (1980). Note in Fig. 9(a) that it takes roughly 90 days for classical LSW to reach its convective depth under average conditions. This is in line with Clarke and Gascard (1983) (who used constant forcing), and confirms the importance of the cyclonic gyre in keeping water parcels trapped in this area long enough to form the product, as noted by those authors.

Southern interior water. The reduced heat loss to the southeast (Fig. 7(b)), together with the lighter *in situ* density of the upper layer in this region, results in a lighter, shallower winter product in the southern interior Labrador Sea (region 2, Fig. 8). While the final density of this product varies more from station to station than for the classical LSW, it is generally centered in the density class between the upper LSW and classical LSW. Mixed-

layer depths are typically 400–700 m, much shallower than the large values observed further north. It should be noted that a few of the stations in this region do produce a product light enough to be upper LSW; this also occurs if the forcing is weaker. However, the θ and S of this lighter product are simply too warm and salty to be the upper LSW source (consistent with our earlier discussion of the warm region in the lateral map of Fig. 3(b) in the southern Labrador Sea). Marked in Fig. 9(b) is the θ–S of the upper LSW eddy observed off Flemish Cap. As shown in Pickart *et al.* (1996) these eddies erode substantially as they progress southward (i.e. quickly becoming warmer and saltier). Thus, at formation in the environs of the Labrador Sea the water must be significantly colder and fresher than that measured in the eddy off Flemish Cap. As seen in Fig. 9(b) (and Fig. 17(b)), this is not the case for the water mass product of region 2, which, therefore, precludes this region from being the source of the upper LSW.

Upper LSW. In both the northern and southern interior regions the waters of the upper layer are too salty to form upper LSW via overturning. Since the coldest and freshest water within the Labrador Sea is found in the Labrador Current, it is only natural to consider the western boundary as the source of the upper LSW. The mixed-layer model reveals that, indeed, there is a narrow band along the upper continental slope where overturning can form the water mass product observed in the downstream eddies. The mechanism by which this occurs can be understood by considering the density section of Fig. 1(c). In this section (which is typical of the region) one sees the downward onshore tilt of isopycnals associated with the main branch of the Labrador Current near the shelf break. On the seaward edge of the front, note that the thickness of the density layer corresponding to the upper LSW (27.68–27.72 kg/m^3) is increased substantially relative to the interior. When heat is removed from the surface, the mixed-layer here at first deepens very slowly due to the fresh salinity cap. However, upon eroding this cap and penetrating the thick sub-surface layer, the overturning quickly progresses to depths on the order of 1000 m (mixing the low salinity water downwards). This is visualized in Fig. 9a (region 3), which shows this rapid increase of the mixed-layer depth, followed by an abrupt leveling-out to a constant level when the end of the thick layer (or the bottom) is reached. Note that the final θ–S is in the range required for the upper LSW eddies. Interestingly, the mixed-layer product here is deeper than in the southern interior Labrador Sea (region 2), even though the initial upper layer density is greater in the interior. This is due to the large isopycnal slope near the boundary (i.e. the thick layer already extends deep), which reflects the baroclinicity of the Labrador Current.

Thus the evolution of the overturning here, and hence the formation of the upper LSW water mass, is intimately tied to the dynamics of the Labrador Current. The potential vorticity structure of the sub-surface front provides a favorable initial condition. The reason why the area of formation is restricted to such a narrow band along the boundary is that farther shoreward the surface layer freshens even more, causing an impenetrable salinity cap (the water here can freeze as well, which also inhibits overturning). Seaward of the shelf break the upper LSW layer shoals and thins (Fig. 1(c)) and hence has little impact on the final product (as discussed above). We note, however, that this narrow formation region is within the core of the Labrador Current and hence is associated with significant southward transport. Because of the narrowness of the region, only a small number of stations in Fig. 6 produced upper LSW, none of them in the southern portion of the domain. We suspect that this is more a matter of station placement than the inability to form this water to the south, although the latter possibility cannot be dismissed.

The time for the upper LSW to reach its equilibrium mixed-layer depth in Fig. 9(a) is 60 days, compared with 90 days for the classical LSW. This suggests that the formation of upper LSW might be less sensitive to the severity of a given winter and hence occur on a more regular basis than classical LSW (which is known to vary inter-annually, e.g. Lazier (1980)). The constancy of the observed upper LSW signal downstream in the DWBC implies that this is the case (Pickart, 1992). This reduced time to form upper LSW is also important with regard to the strong advection in the Labrador Current. In contrast to the western Labrador Sea gyre, which recirculates the water in region 1 (enabling the cooling to act long enough), the Labrador Current advects the surface water equatorward at roughly 20 cm/s (Lazier and Wright, 1993). This raises the question of whether the water resides in the area long enough to form upper LSW. This is answered by noting that the net displacement of a water parcel traveling at this speed for a period of 60 days is 1000 km, which is equal to the distance along the boundary over our domain (Fig. 8). Furthermore, the upper layer temperature and salinity fields in this domain (not pictured) show very little downstream variation in properties along the shelf break in the main branch of the Labrador Current (in contrast to the interior, which shows substantial north–south gradients). Thus, our one-dimensional mixed-layer model is, indeed, reasonable in this strongly advective boundary region, and one could think of the above results as applying to the Lagrangian reference frame.

The idea of convection within the core of the main Labrador Current is new, and observations are certainly needed to investigate such a phenomenon. Indeed, the general concept of overturning within a baroclinic shelf-break current requires further study. In our present work the mixed-layer model is over-simplified, and uncertainties exist regarding the forcing and initial conditions. Despite this, the above-described formation of the upper LSW seems plausible and is consistent with the water mass observations of Pickart *et al.* (1996). Furthermore, there is a bit of direct evidence that this type of winter-overturning does, in fact, occur in the main Labrador Current. During 1987–1988 a set of current meter moorings was occupied in the western Labrador Sea (Lazier and Wright, 1993), one of which was located in the Labrador Current precisely where such convection should occur (within the low potential vorticity layer, Fig. 1(c)). The time series of potential temperature at the 400 and 1000 m instruments are shown in Fig. 10 (the 400 m record ended in mid-winter). In January the temperature at the upper instrument undergoes a fairly sudden and

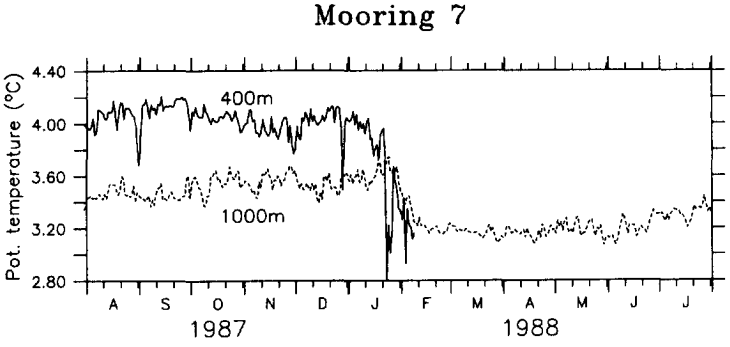

Fig. 10. Time series of potential temperature at mooring M7 in the Labrador Current (see Fig. 1 for a vertical perspective of the mooring and Fig. 6 for a lateral perspective). The solid line is the 400 m record, and the dashed line is the 1000 m record.

drastic drop, followed about 2 weeks later by a similar drop at the lower instrument to the same temperature. While a detailed analysis of these data is beyond the scope of our present study, this sequence certainly suggests that such convective formation of upper LSW can occur in the main branch of the Labrador Current.

MODEL OF EDDY FORMATION

The next important question to be answered is, once the Labrador current is ventilated with new upper LSW, how are the eddies formed, and how do they come to be found seaward of Flemish Cap (Fig. 6)? To address these issues we implemented a four-layer primitive equation numerical model of the two branches of the Labrador Current in the vicinity of Flemish Cap (Fig. 11). Specifically, the model contains the baroclinic main

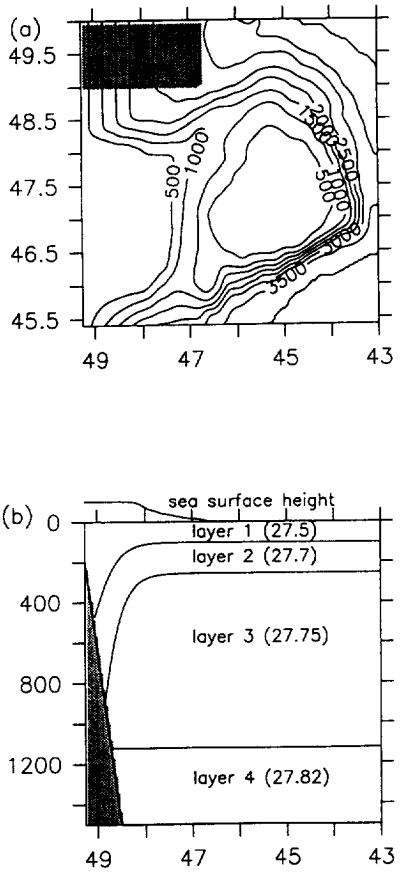

Fig. 11. (a) Model domain and bottom topography. The model is forced within the shaded region through non-conservative terms in the momentum and continuity equations. (b) Vertical section through the model initial conditions at 49.5°N (the density of each layer is indicated). The layer interfaces indicate the location of the main Labrador Current, and the sea–surface elevation marks the position of the offshore deep Labrador Current. (The free surface has been scaled by 1000 for clarity; the change in height across the deep Labrador Current is 0.1 m).

branch located at the shelf break (including the sub-surface low potential vorticity layer) and the barotropic deep branch farther offshore. An inherent assumption here is that to the south near Flemish Cap the upper LSW is isolated from the sea surface. This may be due to subduction under a lighter *in situ* density layer or simply capping-over subsequent to the convection. As detailed below, both the deep Labrador Current and the topography of Flemish Cap play a crucial role in the upper LSW eddy formation process.

Model configuration and forcing

The model we use is based on the Miami Isopycnal Coordinate Ocean Model (MICOM) documented by Bleck *et al.* (1992). It solves the primitive equations of motion using an isopycnal vertical coordinate. This configuration permits accurate treatment of steep and tall bottom topography and vanishing layer thicknesses, and it lends itself well to the consideration of individual water masses. The governing equations are provided in the Appendix; details of the model design and numerics can be found in Bleck *et al.* (1992).

A number of simplifying assumptions and modifications have been made in order to pose the problem in the simplest possible context. The model domain is a periodic channel in the north–south direction with closed, no-slip boundary conditions on the eastern and western boundaries. The model is forced through non-conservative terms in the momentum and continuity equations in the shaded region of Fig. 11(a) (discussed further below). Since the ventilation process is assumed to be over, the flow is made adiabatic by turning off the diapycnal mixing and surface buoyancy forcing. The model temperature and salinity are constant within each isopycnal layer so the model effectively carries only the potential density field. There is also no mechanical forcing of the surface layer (wind stress or wind-induced vertical mixing). The stratification has been chosen such that none of the interior layers outcrops at the surface; however, due to the strong bottom topography and baroclinicity of the main Labrador Current, all of the layers intersect the bottom at some point along the western boundary.

We have chosen to focus the modeling study on the region surrounding Flemish Cap because the topography there causes a splitting of the pathways for the baroclinic Labrador Current (which lies near the outer shelf break) and the wind-driven barotropic Labrador Current (which lies approximately over the 2500 m isobath, Fig. 11(a)). As will be shown, this leads to an exchange of mass between the near-shore baroclinic current and the offshore wind-driven flow. While calculations with a straight coastline indicate that eddies should be formed by the baroclinic Labrador Current to the north of Flemish Cap, the exchange between the coastal regime and the interior wind-driven regime is made most explicit in the vicinity of Flemish Cap where the two currents diverge.

The model domain is a 500 km square with horizontal grid resolution of 4 km (126 × 126 grid points, Fig. 11(a)). The potential densities of the four layers were chosen to be 27.5, 27.7, 27.75 and 27.82 kg/m^3. The uppermost layer denotes the seasonal thermocline, layer 2 is the low potential vorticity water representing the upper LSW, and layers 3 and 4 constitute the intermediate and abyssal ocean. Within the core of the main Labrador Current the first deformation radius is approximately 7.5 m, reasonably well resolved by the model grid.

The initial layer thicknesses (Fig. 11(b)) are consistent with the vertical section of Fig. 1(c). This is formally designated through the interface depths (p_k) as a function of cross-front position (x) as

$$p_k = P_{\max\, k} + 0.5\delta_k[\tanh(x/l) - 1], \tag{1}$$

where $P_{\max\, k}$ is a maximum interface depth, δ_k is the change in interface depth across the Labrador Current, x is the distance from the 500 m isobath, and l is a cross front width. For the calculations presented here, $P_{\max} = 900$, 2600, 1100 and 4000 m; $\delta_k = 800$, 2350, 0, and 0 m; and $l = 40$ km. It should be noted that the upper two layers never reach the maximum depth because they intersect the bottom topography at about 400 and 965 m, respectively. We are particularly interested in the low potential vorticity region of the second layer, which corresponds to the upper LSW. The potential vorticity of this layer increases by about a factor of 4 from the core of the boundary current in to the interior. The maximum velocities in the upper two layers of the boundary current are approximately 22 cm s^{-1} and 8 cm s^{-1}, giving rise to a total transport within the main Labrador Current of 3.0 Sv. This is close to the baroclinic transport of 3.8 Sv estimated further upstream by Lazier and Wright (1993). We note that these initial conditions are designed to represent the basic characteristics of the Labrador Current system and are not meant to yield a detailed prediction of the actual evolution of the flow.

The model is also initialized with a barotropic jet further offshore that represents the deep Labrador Current (Lazier and Wright, 1993; Pickart *et al.*, 1996). This current is defined through the variation in sea surface height as

$$p_s = 0.5\delta_s[\tanh(x_s/l_s) - 1], \tag{2}$$

where p_s is the surface pressure, δ_s is the change in surface pressure across the jet, $x_s = (h - h_0)/\alpha$ is a scaled distance, and l_s is the width scale of the barotropic front. The scaled distance effectively allows the barotropic flow to follow contours of constant depth (or constant f/h in the present f-plane model). The parameters are chosen to be $\delta_s = 1 \times 10^4$, $h_0 = 2500$ m, $\alpha = 1 \times 10^{-4}$, and $l_s = 30$ km. The front is centered over the 2500 m isobath, as found by Lazier and Wright (1993), and has a typical maximum velocity of 20 cm s^{-1} for the topographic slopes around Flemish Cap. The total transport of this offshore barotropic current is approximately 15 Sv.

The model is forced through non-conservative terms in the momentum and continuity equations that restore the model prognostic variables towards the initial layer thickness, surface pressure and balancing geostrophic velocity. These terms are non-zero in only a small upstream region of the model domain (shaded area, Fig. 11(a)). The use of such non-conservative terms allows for specified structure of the boundary currents to flow in to the model domain without having to use technically difficult open boundary conditions. This region acts to convert the outflow conditions at the southern limit of the model domain in to the specified inflow conditions by using the periodic boundary conditions. Spall (1994) used similar non-conservative terms to force an abyssal circulation model with a deep western boundary current.

A passive tracer is also integrated by the model. The tracer is initially zero everywhere in the model domain, and restored towards a value of 1 in the non-conservative region of the baroclinic Labrador Current (west of 48.4°W). This tracer is used to track the signature of water masses; it may be thought of as a proxy for transient tracers, such as CFCs and tritium, of which high concentrations were found in the upper LSW eddies (Pickart *et al.*, 1996). Sub-grid scale processes are parameterized in the model through a Laplacian diffusion of layer thickness, momentum and passive tracers. The coefficients used here were

1.0×10^5 cm^2 s^{-1} for layer thickness and passive tracers, and 1.6×10^5 cm^2 s^{-1} for momentum. Although not excessively tuned, these parameters were chosen to be as small as possible while maintaining computational stability.

Results

Results from a central model calculation of 200 days are presented here, with a number of additional model runs carried out to demonstrate the sensitivity of these results to variations in the configuration. The main branch of the baroclinic Labrador Current remains along the shelf break and flows through Flemish Pass, while the offshore deep Labrador Current flows around Flemish Cap. The main branch is baroclinically unstable as a result of the variations in potential vorticity across the front. The upper two layers have low potential vorticity within the core of the current and high potential vorticity in the surrounding waters, while the intermediate layer has relatively high potential vorticity in the current and low potential vorticity offshore. This structure is seen in the sections of Figs 1(c) and 11(b). Such a change in sign of the cross-front potential vorticity gradient satisfies a necessary condition for baroclinic instability (Pedlosky, 1979).

The front develops unstable meanders, which reach large amplitude by day 25 (Fig. 12). The meanders are beginning to pinch off eddies of large layer thickness (low potential vorticity) from the core of the current. The geostrophic adjustment of these eddies in the more strongly stratified interior results in an anticyclonic circulation with maximum signature at mid-depth and a weaker signature at the surface (Spall, 1995). Several of these large amplitude meanders are visible in the velocity field as anticyclonic circulations of 5–10 cm s^{-1} and layer thickness anomalies of approximately 200 m (Fig. 12). The eddy that has detached near 47.2°W, 48.5°N is just beginning to interact with the barotropic deep Labrador Current, which is visible in the velocity field but not in the thickness field. A long plume of enhanced layer thickness has already been entrained into the deep offshore current and is being advected around Flemish Cap. (We point out that the region of small layer thickness denoted by the closed contours near 45°W, 47°N is due solely to the shallow topography of Flemish Cap, and is not important to the present discussion.)

By day 100 several of the eddies have detached completely from the baroclinic Labrador Current and have been entrained in to the deep Labrador Current (Fig. 13). The eddies vary in diameter from 50 km to nearly 100 km. There are three clearly detached eddies located at 44°W, 44.75°W and 46.2°W, with another just beginning to form at 48°W. At this point the eddies are strongly interacting with the onshore edge of the deep barotropic flow, which inhibits continued movement of the eddies further offshore and rapidly carries them along the topography around Flemish Cap. The eddies are nearly axisymmetric and of sufficient strength to be visible in the velocity field. The region near the entrance to Flemish Pass (where the two branches of the Labrador Current diverge) has been mostly filled with the weakly stratified water that was originally confined to the core of the baroclinic jet.

After 200 days the weakly stratified water has been advected all the way around Flemish Cap by the deep Labrador Current (Fig. 14). Eddies are still visible, but have been considerably weakened by lateral shear and diffusion. The horizontal shear of the deep Labrador Current has stretched the initially circular eddies into elongated, plume-like features as they have been advected around the topography. There is now very little signature of the eddies in the velocity field, but the thickness anomalies are still approximately 50–100 m. The location, scale and amplitude of these low potential

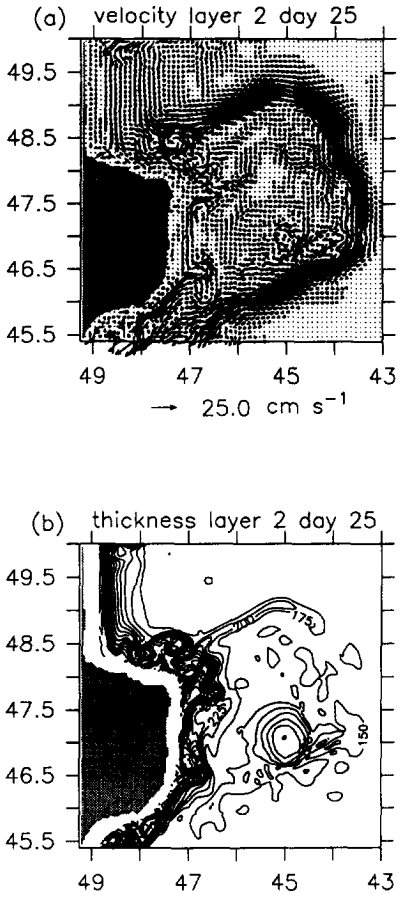

Fig. 12. Model fields for layer 2 on day 25. (a) Horizontal velocity (only every other point is plotted). (b) Layer thickness (the contouring is omitted where the layer thickness vanishes due to topography, for clarity).

vorticity patches in the plume are remarkably similar to the observations of the upper LSW lenses described in Pickart *et al.* (1996). The baroclinic Labrador Current continues to spawn eddies near the formation region, as is evident in the thickness field.

The passive tracer that is introduced into the model domain within the baroclinic Labrador Current in the northwest corner is shown in Fig. 15 for model day 200. There is clearly a splitting of the tracer, indicating that some of the water mass carried by this current indeed gets diverted to deep water via the eddy formation process and advected around the outside of Flemish Cap by the deep Labrador Current. The patchiness of the eddies is also evident in the tracer field, although the leading eddy contains no tracer because it was formed before the tracer was advected that far equatorward (the initial value of the tracer was zero in the interior). The lateral shear of the deep jet increasingly suppresses the spatial patchiness well downstream of the formation region. The early signature of future eddy formations is evident in the tracer field near the formation region at 48°W.

The fraction of water in layer 2 of the baroclinic jet that gets diverted around Flemish Cap

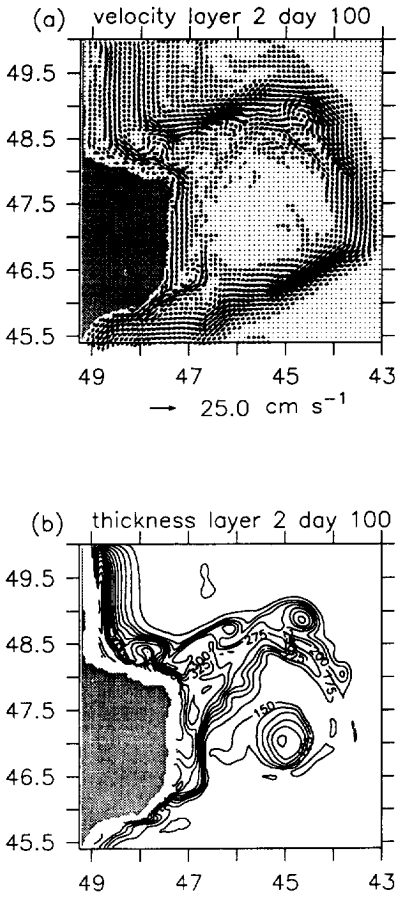

Fig. 13. Same as Fig. 12 for day 100.

has been calculated by comparing the tracer flux through the three sections shown in Fig. 15. Section A measures the total amount of tracer being advected into the region, while sections B and C calculate the amounts that are transported through Flemish Pass and to the outside of Flemish Cap, respectively. The fluxes through the three sections are shown as a function of time in Fig. 16(a). After an initial spin-up period of about 100 days, approximately one-third of the total tracer transport in layer 2 is diverted around Flemish Cap, with the remainder flowing through Flemish Pass (a calculation based on mass transport yields a similar splitting of the main Labrador Current).

The barotropic deep Labrador Current is crucial to this entrainment and diversion of the low potential vorticity Labrador Current water. This is demonstrated by the tracer transports shown in Fig. 16(b) for a case with no deep Labrador Current. The transport through section C is now nearly zero, while the transport through Flemish Pass continues to grow over the duration of the experiment. The difference between the transport into the model domain and that carried through sections B and C is accounted for by an accumulation of tracer just north of Flemish Pass in the form of anticyclonic eddies. They continue to form, as in the previous case, but there is no mechanism to take them away from

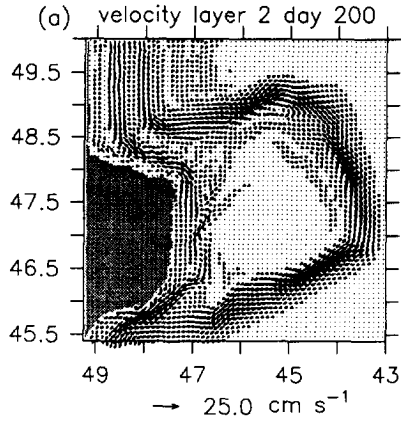

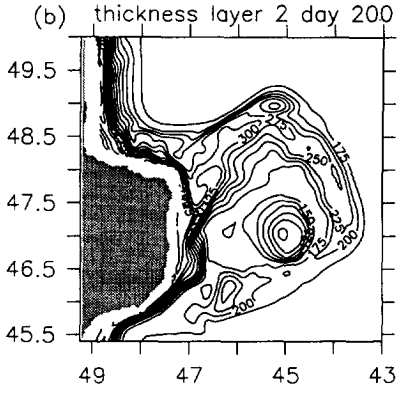

Fig. 14. Same as Fig. 12 for day 200.

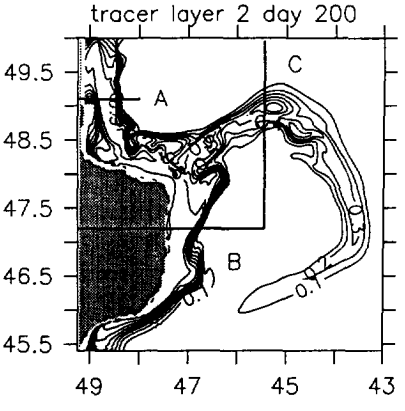

Fig. 15. Passive tracer marking the Labrador Current water in layer 2 on day 200.

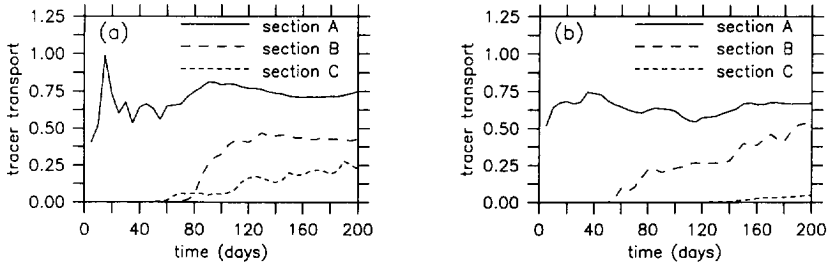

Fig. 16. Tracer transport through sections A, B and C (locations shown on Fig. 15). (a) Calculation with deep Labrador Current and (b) calculation with no deep Labrador Current.

the formation region so they simply accumulate there. The gradual growth of the tracer transport through the pass indicates that the rate of accumulation (or eddy formation) is decreasing. This is because the build up of low potential vorticity waters offshore of the baroclinic Labrador Current stabilizes the current and suppresses future meander growth. This is also seen to a lesser extent in the case with the deep Labrador Current (Fig. 14(b)).

While the transport around Flemish Cap is dependent on the existence of the deep current, it is relatively insensitive to the exact position of the deeper flow. A series of calculations have been carried out in which the center position of the deep Labrador Current has been varied from the 2250, 2500 and 2750 m isobaths. The average tracer transport in each case is quite similar: approximately one-third of the total transport gets diverted around Flemish Cap, although there are high frequency variations associated with the passage of individual eddies. This lack of sensitivity is important because, while it is believed that the deep Labrador Current exists at these latitudes, its exact position and structure are not well known. We note that there are no appropriate measurements to verify this detrainment mechanism. However, such a diversion of transport at Flemish Pass is consistent with the volume flux estimates of Loder *et al.* (in press).

EXTREME FORCING

The final issue that we address in this work is the sudden appearance in the 1990s of newly-ventilated classical LSW downstream in the DWBC. As discussed earlier, no high-CFC water of this density was observed in the DWBC over the first decade that CFCs were measured. Pickart *et al.* (1996) discuss the first occurrence of newly-ventilated lenses of this water in the DWBC in 1991–1992. This equatorward flux seems to have increased over the past few years, and a 1994 survey suggests that nearly all of this density layer of the DWBC in the mid-Atlantic Bight contains such new water. At the same time, Sy *et al.* (1997) report a similar appearance of recently formed classical LSW in the Irminger Sea, suggesting a much more rapid eastward transit of this water than previously observed (Read and Gould, 1992). These observations indicate that something in the sub-polar system has changed in the last several years that has "opened the floodgates", allowing classical LSW to exit rapidly from the Labrador Sea. We suggest here that this is a consequence of classical LSW being formed on the southern fringe of the Labrador Sea (i.e. in region 2 above) due to extreme forcing, which allows for a much easier escape to the interior North Atlantic.

Starting in 1989–1990 there has been a succession of severe winters in the Labrador Sea

(documented, for example, by particularly low air temperatures at Iqaluit on southern Baffin Island). Such repeated extreme air–sea forcing has significantly increased the density of the classical LSW product in region 1, to the point where it is now at its densest extreme over the 30-plus-year modern record. This recent change has been chronicled by the yearly springtime occupation of the WOCE AR7W hydrographic line, which crosses the central Labrador Sea (region 1, Fig. 8). The density increase is due mainly to a steady decline in the temperature of the convective product. While our mixed-layer model uses historical data and certainly cannot be used to investigate a series of winters, it is none the less instructive to run the model with the extreme forcing curve of Fig. 7(a).

This was done first for the stations in the central part of the western Labrador Sea gyre in region 1. The extreme forcing here produces a deeper, denser product (Fig. 17(A)), where the change in density is due primarily to a decrease in temperature (consistent with the recent AR7W observations). Recall, however, that this water is recirculating within the cyclonic gyre (Fig. 8), and hence we expect that it cannot easily exit the region. It remains unclear precisely how and how fast such newly-formed water in the central Labrador Sea does spread to the interior. Recent work suggests that this occurs by the action of baroclinic eddies subsequent to the convection (e.g. Visbeck *et al.*, 1996). It seems unlikely, however,

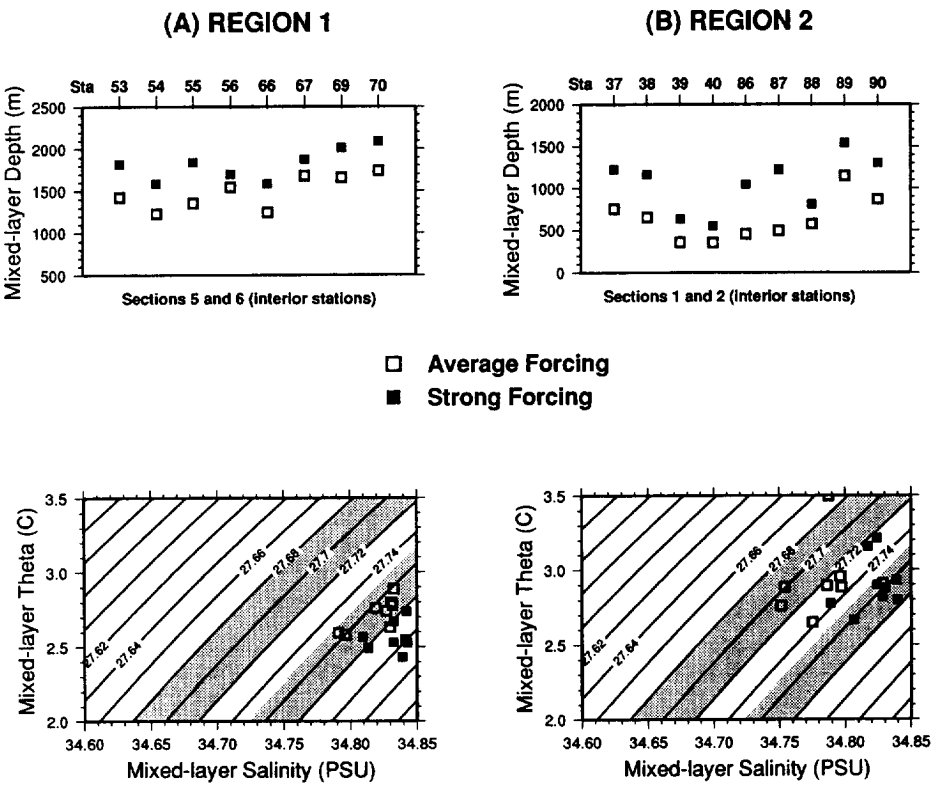

Fig. 17. Comparison between average and extreme forcing of the mixed-layer model. The upper panel is the final mixed-layer depth, the lower panel is the final θ–S. The density ranges of the upper LSW and classical LSW are indicated by shading. (A) Region 1 in the central part of the gyre. (B) Region 2 towards the south.

that this process can account for the short time scale over which the recent classical LSW has appeared downstream in the DWBC. In addition, it is not obvious that this eddy transfer would become significantly more efficient due to the enhanced air–sea forcing in the last few years. Hence, while extreme forcing seems to produce an extreme version of classical LSW, it none the less remains "trapped" to some degree within the cyclonic gyre.

In contrast to region 1, the water mass product formed in region 2 outside the gyre has a much more direct link to the interior North Atlantic. Inspection of Fig. 8 shows a weak anticyclonic flow to the southeast, which is an influence of the nearby North Atlantic Current. Inshore of this is a band of minimum dynamic height (nearly stagnant flow) adjacent to the western boundary current. Thus, the newly-formed water in region 2 could be readily entrained into the equatorward-flowing DWBC and advected out of the Labrador Sea. Likewise a direct advective path exists to the Irminger Sea via the edge of the North Atlantic current. As presented earlier, the typical water mass product in this region is lighter than classical LSW and confined to shallow depths. However, when subject to extreme forcing, the mixed-layers can deepen to 1000–1500 m and, by mixing salinity from below, increase the density of the layer into the range of classical LSW (Fig. 17(B)). Note that this is in contrast to region 1 where the density change was governed predominantly by temperature. Thus, the "severe winter" classical LSW product in region 2 has salinity comparable to that in region 1, but is warmer and hence a bit lighter (compare Fig. 17(A) and (B)). It is also worth noting that the severe winter version of classical LSW in region 2 is nearly identical in T–S to the average winter classical LSW in region 1 (again consult Fig. 17(A) and (B)).

There is, in fact, evidence that such formation of classical LSW on the southern fringe of the Labrador Sea is the reason for the sudden appearance of this water type in the DWBC. As discussed in Pickart *et al.* (1996) the observed lenses of classical LSW in the DWBC become warmer and saltier as they progress downstream due primarily to isopycnal mixing. The conservative nature of the density thus offers insight as to the time of formation of the water. The evolution of the classical LSW in region 1 over the past 8 years (from the AR7W data) is shown in Fig. 18, revealing the general decline in temperature and increase in density as of late. These points denote the potential density of the temperature minimum of the LSW within the cyclonic gyre. This same quantity was computed for the downstream lenses in the DWBC, and the values are also shown in Fig. 18. Note both the increase in temperature (due to the downstream moderation) and the constancy of the density of these points. Finally, as part of the 1991 late winter survey (EN223) there were two stations occupied within region 2 (marked on Fig. 8). Both these stations revealed evidence of convection to roughly 1500 m with comparable values of θ, S and low potential vorticity (not shown). Again, we computed the same quantity for these stations, whose value is included in Fig. 18.

Figure 18 implies that the downstream lenses of classical LSW in the DWBC were formed either in the central Labrador Sea in 1990 (region 1), or the southern Labrador Sea in 1991 (region 2). The latter is most likely true. Recall that the DWBC lenses represent data from two years (1991 and 1992). If they originated from region 1 then one should see an offset in the density of the lenses corresponding to the offset in the AR7W data from 1990 to 1991. There is no such trend (Fig. 18). Also, if region 1 were the formation site this would imply a short (i.e. 1-year) lag from the cyclonic gyre to the DWBC on a regular basis (since classical LSW is regularly formed in region 1). As pointed out this is not observed, and it is not likely via the eddy transport mechanism out of the gyre.

It is more likely that the lenses within the DWBC contain water from region 2 formed

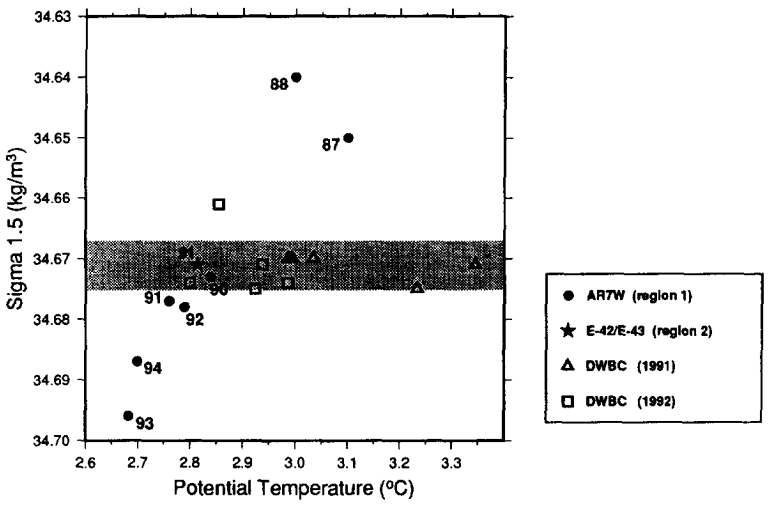

Fig. 18. Potential density (referenced to 1500 db) corresponding to the minimum in potential temperature of the classical LSW. The solid dots are an average of all available data within region 1 for each given year (1987–1994), mostly from the AR7W cruises. The shaded star is an average of the two EN223 stations in region 2 in 1991. The open symbols are lenses of classical LSW observed downstream in the DWBC in 1991 and 1992 (from Pickart *et al.*, 1996). The shading denotes the standard deviation of the DWBC lenses.

earlier the same year. The observed 1991 Labrador Sea products in regions 1 and 2 differ in temperature only (the water mass in region 2 is warmer and lighter), consistent with the model results. We can assume from Fig. 18 that in region 2 water of comparable density was formed in both 1991 and 1992 (since this was true for the AR7W data to the northeast), which explains the similar density for all the downstream lenses. In addition, the circulation in region 2 allows for such a rapid expulsion; yet only under extreme conditions (such as those occurring in the early 1990s) will the exported product be classical LSW. We note that for a classical LSW lens to appear by April at the two southern-most sections of EN223 (Fig. 2) implies an advective speed of 10–25 cm s^{-1} if formed in early winter. Such strong currents are in line with the absolute velocity data of Pickart *et al.* (1996). At the same time it is not difficult to imagine short convective times after repeated harsh winters. Clearly more evidence is needed to document our assertions; however, these results suggest a remarkably fast flushing time for classical LSW under severe forcing—on the order of months. The historical CFC data imply that under normal conditions the spreading time is as long as a decade. Such a drastic change surely has strong consequences regarding the ventilation of this density layer in the North Atlantic. An understanding of such rapid response mechanisms will be necessary to interpret changes in the thermohaline circulation away from water mass transformation regions and to relate such changes to variability in the atmospheric forcing.

SUMMARY

New aspects of the ventilation within the western sub-polar gyre have been investigated using recent observations in conjunction with regional numerical modeling. Our results emphasize the importance of the boundary current system in the replenishment of

intermediate waters to the North Atlantic. We have demonstrated with a simple mixed-layer model that overturning to 1000 m can occur within the main branch of the Labrador Current, forming a water mass that is fresher and lighter than the classical LSW originating in the interior Labrador Sea. This water mass (termed upper LSW) is formed only in a narrow band along the upper continental slope seaward of the ice edge, where the potential vorticity structure of the main Labrador Current provides a favorable initial condition. The θ–S of the upper LSW is consistent with that contained in the sub-mesoscale eddies observed seaward of Flemish Cap by Pickart *et al.* (1996). Lateral property maps constructed using our *in situ* data, together with these mixed-layer results, indicate that the western boundary can be the only source of this water.

A regional numerical model of the circulation near Flemish Cap demonstrated clearly how upper LSW eddies can be formed by the main branch of the Labrador Current and subsequently transported offshore. The potential vorticity structure of the main Labrador Current again plays a key role, causing the current to be baroclinically unstable and form mid-depth eddies after only 25 days. The eddies then become entrained in to the offshore deep Labrador Current which carries them around Flemish Cap, while the main branch of the Labrador Current remains trapped to the boundary and flows through Flemish Pass. The narrow width of the offshore jet shears the entrained eddies as they advect and causes them to erode quickly, consistent with the observations of Pickart *et al.* (1996). The model suggests that as much as one-third of the transport of the baroclinic Labrador Current gets diverted to the offshore jet. This represents a significant exchange between buoyancy-driven and wind-driven flow, the latter of which provides more direct communication with the interior.

Finally, we have presented a plausible scenario which explains the sudden flux of classical LSW into the sub-tropical North Atlantic via the DWBC. This flux has coincided with a series of harsh winters in the Labrador Sea, and our mixed-layer model shows that under severe forcing classical LSW can be formed on the southern fringe of the Labrador Sea. This offers direct access to the south (via the DWBC) and east (via the North Atlantic Current). A comparison of the 1991–1992 DWBC data with time-series information from the Labrador Sea supports our scenario, and implies that under these conditions classical LSW can exit the Labrador Sea the same year it is formed. This is drastically shorter than under normal conditions.

Acknowledgements—R.P. would like to acknowledge Allyn Clarke for providing the code for the mixed-layer model, and for use of the 1978 CSS *Hudson* data. Terry McKee helped with numerous aspects of the data management and processing. M.S. acknowledges Rainer Bleck for providing the original source code for the general circulation model. This work was supported by NSF grant OCE-90-18409 (R.P.), NOAA grant NA36GP0309 and ONR contracts N00014-90-J-1490 and N00014-93-1-0572 (M.S.).

REFERENCES

Bleck, R., Rooth, C., Hu, D. and Smith, L. (1992) Salinity-driven thermohaline transients in a wind- and thermohaline-forced isopycnic coordinate model of the North Atlantic. *Journal of Physical Oceanography*, **22**, 1486–1505.

Caruso M. J., Singh, S., Kelly, K. A. and Qiu, B. (1995) Monthly atmospheric and oceanographic surface fields for the western North Atlantic: December 1986–April 1989. WHOI Technical Report WHOI-95-05, 69 pp.

Clarke, R. A. and Gascard, J. C. (1983) The formation of Labrador Sea water. Part I: Large-scale processes. *Journal of Physical Oceanography*, **33**, 1764–1778.

Koltermann, K. P. (1995) Is the sub-polar gyre in the North Atlantic spinning up? *Annales Geophysicae. Proceedings of the European Geophysical Society*, **13**(supplement II), C–229.

Lazier, J. R. N. (1973) The renewal of Labrador Sea water. *Deep-Sea Research Part I*, **20**, 341–353.
Lazier, J. R. N. (1980) Oceanographic conditions at Ocean Weather Ship *Bravo*, 1964–1974. *Atmosphere-Ocean*, **3**, 227–238.
Lazier, J. R. N. (1988) Temperature and salinity changes in the deep Labrador Sea, 1962-1986. *Deep-Sea Research Part I*, **35**, 1247–1253.
Lazier, J. R. N. and Wright, D. G. (1993) Annual velocity variations in the Labrador Current. *Journal of Physical Oceanography*, **23**, 559–678.
Loder, J. W., Pettie, B. and Gawarkiewicz, B. (1997) The coastal ocean of northeastern North America (Cape Hatteras to Hudson Strait). *The Sea*, in press.
Moore, G. W. K. (submitted) On the spatial and temporal variability of surface heat fluxes over the North Atlantic during winter. *Journal of Climate*, submitted.
Pedlosky, J. (1979) *Geophysical Fluid Dynamics*. Springer-Verlag, New York, 624 pp.
Pickart, R. S. (1992) Water mass components of the North Atlantic deep western boundary current. *Deep-Sea Research*, **9**, 1553–1572.
Pickart, R. S., Smethie, W. M., Jr., Lazier, J. R. N., Jr., Jones, E. P. and Jenkins, W. J. (1996) Eddies of newly formed upper Labrador Sea water. *Journal of Geophysical Research*, **101**, 20,711–20,726.
Read, J. F. and Gould, W. J. (1992) Cooling and freshening of the sub-polar North Atlantic ocean since the 1960s. *Nature*, **360**, 55–57.
Spall, M. A. (1994) Wave-induced abyssal recirculations. *Journal of Marine Research*, **52**, 1051–1080.
Spall, M. A. (1995) Frontogenesis, subduction, and cross-front exchange at upper ocean fronts. *Journal of Geophysical Research*, **100**, 2543–2557.
Sy, A., Rhein, M., Lazier, J. R. N., Kollermann, K. P., Meincke, J., Putzka, A. and Bersch, M. (1997) Surprisingly rapid spreading of newly formed intermediate waters across the North Atlantic ocean. *Nature*, **386**, 675–679.
Talley, L. D. and McCartney, M. S. (1982) Distribution and circulation of Labrador Sea water. *Journal of Physical Oceanography*, **12**, 1189–1204.
Thompson, K. R., Lazier, J. R. N. and Taylor, B. (1986) Wind-forced changes in Labrador Current transport. *Journal of Geophysical Research*, **91**, 14261–14268.
Visbeck, M., Marshall, J. and Jones, H. (1996) Dynamics of isolated convective regions in the ocean. *Journal of Physical Oceanography*, **26**, 1721–1734.
Wallace, D. W. R. and Lazier, J. R. N. (1988) Anthropogenic chlorofluoromethanes in newly formed Labrador Sea water. *Nature*, **332**, 61–63.
Williams, R. W., Spall, M. A. and Marshall, J. C. (1995) Does Stommel's mixed layer demon work? *Journal of Physical Oceanography*, **25**, 3089–3102.

APPENDIX

The MICOM model solves four prognostic equations for the isopycnal layer averaged quantities of horizontal momentum, layer thickness, and conservation equations for temperature and salinity. The horizontal momentum equation, with no interfacial stresses or cross-isopycnal mass flux, simplifies to

$$\frac{\partial \mathbf{v}}{\partial t} + \nabla\frac{\mathbf{v}^2}{2} + (\zeta + f)\,\mathbf{k} \times \mathbf{v} + \nabla_\alpha M = +(\Delta p)^{-1}\nabla \cdot (A\,\Delta p \nabla \mathbf{v}) + (\mathbf{v}^* - \mathbf{v})/\gamma \tag{3}$$

where $\mathbf{v} = (u,v)$ is the horizontal velocity vector, p is the pressure, k is the vertical unit vector, $\zeta = \partial v/\partial x - \partial u/\partial y$ is the relative vorticity, $M = gz + p\alpha$ is the Montgomery potential, α, is the specific volume of the layer (constant), Δp is the pressure thickness of the layer, and A is an eddy viscosity coefficient. An additional term has been added to the standard momentum equations that relaxes v towards a specified value $\mathbf{v}^*$ with time constant $\gamma = 5$ days. The f-plane approximation is used here, with $f = 1.0 \times 10^{-4}$.

In the absence of cross-isopycnal mass fluxes, the continuity equation is represented as a prognostic equation for the layer thickness Δp,

$$\frac{\partial \Delta p}{\partial t} + \nabla \cdot (\mathbf{v}\Delta p) = (\Delta p^* - \Delta p)/\gamma. \tag{4}$$

The layer thickness is also forced through a relaxation towards a specified value Δp^* with time constant γ. The forcing velocity $\mathbf{v}^*$ is in geostrophic balance with the pressure field calculated from Δp^* using the hydrostatic relation.

For the present application with no surface forcing, no cross-isopycnal mass flux, and uniform temperature and salinity within each layer the conservation equations for these thermodynamic variables maintain constant values within each layer and, thus, are not presented here. The complete model equations and details about the numerical methods used to integrate the equations can be found in Bleck *et al.* (1992).